# Analysis of the environmental and occupational impact of airborne nanoparticles in controlled scenarios

**Raquel Jiménez Prieto**

**Master Degree in Nanostructured Materials for Nanotechnology Applications**

September 2017

FINAL MASTER PROJECT
Directed by

Dra. Pilar Lobera González

Dr. Francisco Balas Nieto

Overseer: Professor Jesús Santamaría Ramiro

Chemical Engineering and Environment Technologies Department

Institute of Nanoscience of Aragon

Science Faculty

ZARAGOZA UNIVERSITY

# ACKNOWLEDGMENTS

*That is it. It is finished. A whole year of tough work has ended, and I am ready for the next stage. I would like to thank everybody who has made this journey possible.*

*First of all, thanks to my project directors, Dra. M. Pilar Lobera, Dr. Francisco Balas and Professor Jesús Santamaría, for giving me the chance to work, develop and guide this project.*

*Thanks to Dr. Enrique Navarro from Instituto Pirenaico de Ecología for making possible to develop and guide part of this project. Special thanks to Dra. Maria del Carmen Sancho for all her help at the laboratory and hard work.*

*Thanks to all members of NFP group, that in one way or another have shared their knowledge, taught me and help me in the laboratory. Specially to Dra. Nuria Navascues, Dr. Teobaldo Torres and Dr. Carlos Cuestas.*

*A huge thanks to my master in the lab, Dr. Alberto Clemente, for his great support and energy (and his patience with my changing of units). It was nice working with you. As well as my lab partners and office partners, I had a great time with you guys.*

*And last but not least, a huge thanks to all my friends and family, specially my parents and sister. Thanks to Šarūnas, for being in the good and bad moments and for following me everywhere I crazily plan, always.*

*To all of you, THANK YOU.*

## *Abstract*

*Nanotechnology has become indispensable in the daily life. Nanomaterials are present in a lot of products, such as cloths, cosmetics, food industry and medicines among others. In the last decades, the production of nanomaterials has increased and so the exposure to such nanomaterials to workers and even customers.*

*Moreover, it would be necessary to distinguish the ENMs from natural nanomatter that is already in the environment. In order to do that, labelling techniques have been used, particularly fluorescent labelling applied in $SiO_2$ nanoparticles, which is one of the most used ENMs (mobile phones, cosmetics...etc.).*

*Most of the researches are focused on the study of harmful ENMs uptaken through respiratory or ingestion route, but, what about the harm effects through cutaneous route? In this project surface contamination has been assessed using fluorescent $Ru(phen)_3$:$SiO_2$ NPs.*

*Not only that, but it is necessary to catalogue these engineered nanomaterials (ENMs) and test the environmental, health and safety impact. Once ENMs are released into the environment, they suffer several abiotic and biotic interactions so it is not possible to know their fate and disposition. In this project, the toxicity of $Ru(phen)_3$:$SiO_2$ NPs have been tested in Chamydomonas reinhardtii; and aging process have been assessed within a case study focused on Ebro River basin physicochemical properties.*

# INDEX

# 1. INTRODUCTION

Nanotechnology is a broad interdisciplinary area of research, development and industrial activity that has been growing rapidly worldwide for the last decades. It can be used in physics, chemistry, biology, engineering and electronic processes, materials, applications and concepts in which the defining characteristic is one of size [1]. It involves the manufacture, processing and application of materials that are in the size range of nanometers.

Nanostructured materials are attractive due to their extremely small size, so they have a much greater surface area than the same mass of materials at the macro-scale, developing different properties than the same material at the macro-scale. This allows them to be used in new ways, to bring about new effects in larger structures of which they are part, e.g. the 'lotus effect' of surfaces [2]. At nanoscale, quantum effects are more important in determining the properties and characteristics of the material. Of particular interest are nanoparticles (NPs), considered in general to be substances below 100 nm in size in one or more external dimensions [3]. They can present different shapes and can also exist in fused, aggregated or agglomerated forms [4]. Moreover the small size provides a greater surface area so it can have major toxicological consequences [5].

In the last decades, the production of engineered nanomaterials (ENMs) has increase and both EU and USA have identified the nanotechnology as a Key Enabling Technology (KET), that drives the sustainable growth of the society. New applications and properties have been developed thanks to nanotechnology [6, 7, 8].

Nanomaterials are therefore believed to contribute substantially to innovativeness, economic growth and employment [2]. Nanoproducts have hit the market long time ago. The first inventory of commercial nanoproducts was compiled by Maynard and coworkers in 2006 and it contained 300 items. Only three years later, the Woodrow Wilson International Center published an inventory with over 1600 products and a visit to the Nanotechnology Products Database [9]. Today, it is produced well above 6400 items. The economic impact is huge: *Lux Research* valued the nanotech market at 339000 million dollars in 2010, and more than doubled in two years, to reach 731000 MM $ in 2012. Projections for 2018 are in the region of 4000000 MM$ (four trillion) [10]. It also increases the number of workers exposed or likely to be exposed to ENMs, as well as the consumers and environmental; so the exposure to ENMs should be evaluated.

Titanium dioxide ($TiO_2$), silicon dioxide ($SiO_2$), and zinc oxide (ZnO) are the most produced nanomaterials worldwide (on a mass basis). However, silver nanoparticles are the most popular

advertised nanomaterial in the Consumer Products Inventory (CPI), which is present in more than 438 consumer products (24%). On the other hand, one of the most studied nanomaterials has been structures based on silicon dioxide ($SiO_2$) or commonly named silica. In fact, the majority of nanostructured bulk materials (57%) are silicon-based nanomaterials (e.g., computer processor parts, mobile devices) (Figure 1) [11]. This compound is formed by tetrahedral $SiO_4$ units interconnected. Silica occurs naturally in the earth, and it is a component of many construction and manufacturing materials. It is a health hazard only when it is airborne, and crystalline silica particles are constantly inhaled [12]. Thanks to its versatility, non-toxicity, biocompatibility and wide range of applications, researches based on this material has growth in the last years.

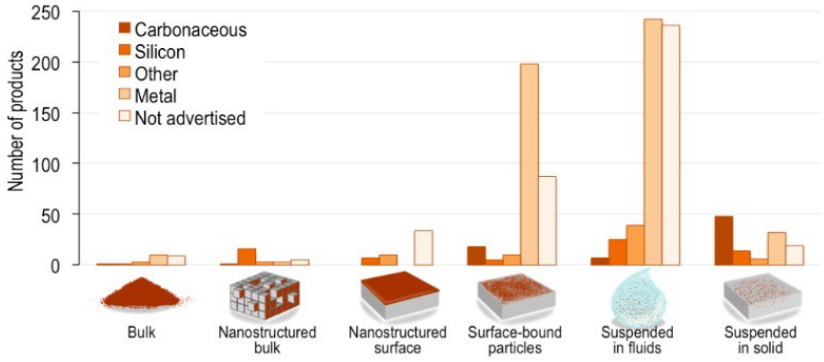


**Figure 1. Locations of nanomaterials in consumer products for which a nanomaterial composition has been identified. (Adapted image [11])**

However, the very novel properties that make nanomaterials useful, may also give rise to health and environmental risks. Some nanomaterials have been shown to have harmful health effects, and there is also a growing concern regarding their spread in the environment [13, 14]. As a consequence, there is already pressure for tighter regulation of nanotechnology and calls for better controls in the handling and disposal of nanomaterials. Indeed, European institutions and organizations have been at the forefront of efforts to ensure safe and practical implementation of nanotechnology. Even though there are many studies about toxicological and environmental characteristics of ENMs, still not yet clear how it can affect humans and environment [15].

While much of the exposure assessment and toxicology literature to date has focused on inhalation exposure, the primary pathway of concern in most occupational settings, there is also need to investigate other potential exposure pathways. Cutaneous exposure to engineered nanomaterials may occur through intentional use of consumer products (e.g. sunscreen, cosmetics) and therapeutic applications (e.g. drug delivery) or unintentionally, including in occupational setting where nanoparticles or nano-enabled products are manufactured, used or handled. Indeed, manual

handling of nanoparticles is a basic task of most nanomaterial research; thus workers are exposed every day to such materials which can have adverse health effects [16].

Many variables were found to affect the extent of particle release of airborne nanoparticles including temperature, room conditions, work practices, type and quantity of material being handled, etc [17]. In these scenarios, surface sampling protocol is crucial and it can be used for measurements of the skin, inner and outer clothing or protective item layers, and surface contaminant layer [18, 19]. This information is useful in identifying material characteristics, calculating exposure point concentrations, and/or evaluating the effectiveness of protective equipment or a decontamination process.

On the other hand, the increasing presence of nanotechnology in the marketplace entails an expanding probability of finding ENMs in the environment. Although the amount of released ENM into the environment is relatively small compared to conventional chemicals, the potential release of nanomaterials will noticeably grow as the production and applications of nanomaterials increase [20]. Figure 2 shows how substances move through air, water, soil and living organism. It is a general biogeochemical cycle, where everything is connected in a way that, when a pollutant or ENM is introduced in the ecosystem, everything is polluted due to the energy and nutrients flow.

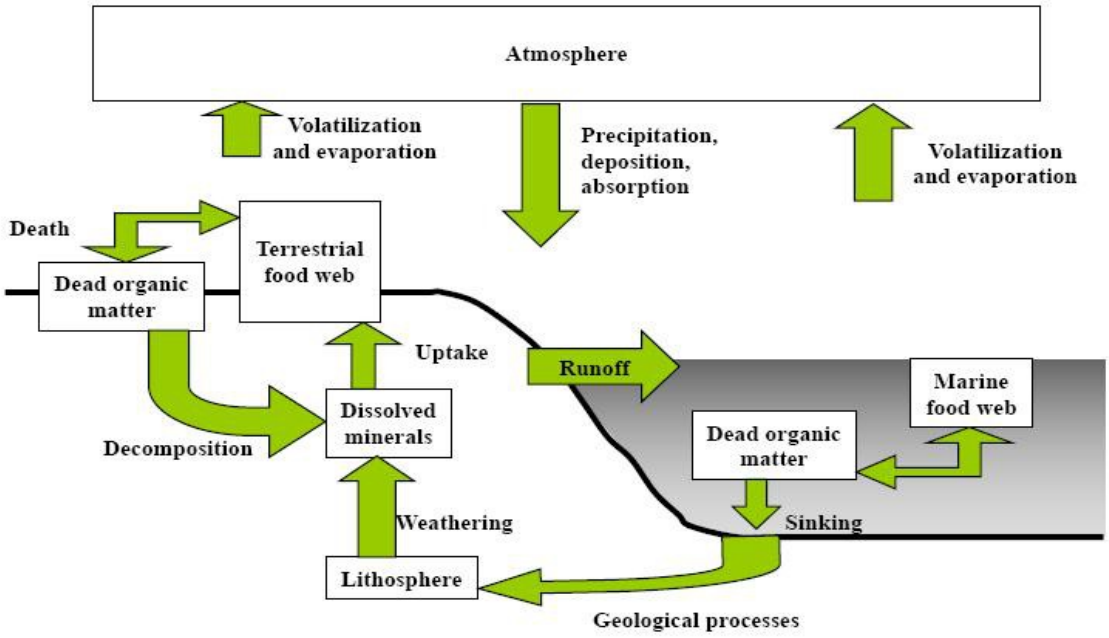


**Figure 2. Scheme of biogeochemical cycling.**

Ecosystems are highly complicated systems where the nanomaterials introduced go through a sequence of abiotic and biotic interactions, as shown in Figure 3. Several studies in the literature have highlighted that, as nanomaterials aging, they can undergo photochemical transformations, oxidation and reduction, dissolution, precipitation, adsorption and desorption, combustion, abrasion and biotransformation, among other biogeochemical processes [21]. However, fewer efforts have been made to know how these changes affect the physicochemical properties of the nanomaterials. Nanomaterials aging is expected to be rapid, even under environmental conditions. With the consequence that pristine ENMs (as synthesized) are never really encountered under natural environmental conditions. The question is still whether ENMs will leave an environmental heritage.

Nanoparticles unique physicochemical properties are often the reason for their increased use in products; however, these same unique properties have prompted concern that physiological responses will be elicited in living systems by interaction with these materials. As the nanomaterial interacts with the environment or organisms, it is important to know how its properties have changed during their aging process.

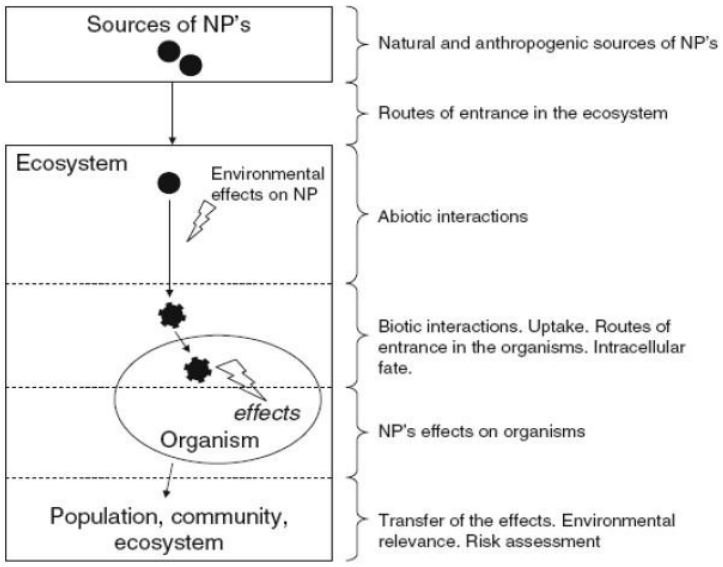


**Figure 3. Scheme of environmental effects on the nanoparticles.**

Despite of the effort to assess the *Environmental, Health and Safety* impact of ENMs, it still a challenge. In a real-life exposure assessment (in occupational and environmental scenarios) the concentration of ENMs under consideration will have to be determined [22]. The main difficulty is related to the fact that the proportion of ENMs in relation to background nanosized matter is likely to be extremely low (in the ppm range or lower), requiring extremely sensitive sampling and

analysis methods. Moreover those ENMs are usually mixed with other nanomaterials, similar in size and properties, which are already present in the environment. Hence, it is necessary to identify and discriminate ENMs from environmental samples. One possibility is labelling the ENMs using specific tags that are not present in the sampling environment [23]. This approach should enable study the fate of the nanomaterials in environmentally and occupationally relevant scenarios (e.g. air, water or solid surfaces for instance). Fluorescent dyes [24], radioactive tracers [25], isotopic labelling [26], rare earth elements [23] and catalytic activity [27] have been proposed for the labelling of nanoparticles in environmental, health and safety applications.

In this project, stable fluorescent labelled nanoparticles based on $SiO_2$ have been synthesized by *sol-gel* process obtaining a colloidal suspension of amorphous solids in a liquid. It has been incorporated and stabilize innocuous fluorescent molecules of Dichlorotris(1,10-phenanthroline)ruthenium(II) hydrate [28], shown in Figure 4. These fluorescent nanoparticles were used to assess the exposure to engineered nanomaterials in occupational setting and their environmental implications.

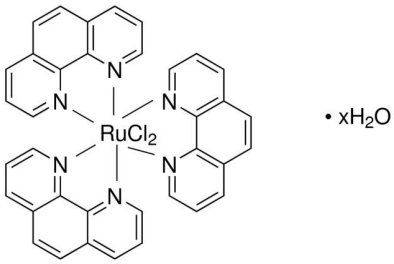


**Figure 4. Chemical structure of $Ru(phen)_3$ and appearance of $Ru(phen)_3$:$SiO_2$ NPs.**

# 2. OBJECTIVES

The core idea of this Master Final Project is to assess the safety and environmental impact of ENMs. Specifically, cutaneous exposure to engineered nanomaterials in occupational setting will be considered and their environmental impact will be studied mimicking real exposure scenario.

To that end, fluorescent labelled $SiO_2$-based nanoparticles will be used as tracers to evaluate the surface contamination in the workplace. This approach might lead to better and earlier identification of ENMs in complex matrices, and therefore it will enable the development of novel risk assessment strategies for the application of nanotechnologies.

Last but not least, the environmental implications of these fluorescent labelled $SiO_2$ nanoparticles will be assessed in *Chlamydomonas reinhardtii* using fluorimetry; and the aging process of $Ru(phen)_3$:$SiO_2$ nanoparticles in environmentally relevant conditions will be addressed in a case study focused in Ebro River basin, as real-life exposure scenario.

# 3. METHODOLOGY

## 3.1 Chemicals

To perform the synthesis of $Ru(phen)_3$: $SiO_2$ nanoparticles, Tetraethyl orthosilicate (TEOS, 98%, Sigma Aldrich), and ethanol (EtOH, 99%, Sigma Aldrich) were used as-received. Milli-Q water® type II (Millipore, Billerica, MA) and ammonium hydroxide ($NH_4OH$, 25–28% solution in water, Sigma Aldrich) were used as reagents for the hydrolysis of silicate precursors. The fluorescent label tris(1,10-phenanthroline)ruthenium(II) chloride hydrate ($Ru(phen)_3Cl_2 \cdot H_2O$, 98%, Sigma Aldrich) was used without previous purification.

*Chlamydomonas reinhardtii* were cultured in Talaquil, which is model fresh water medium, a complete growth medium containing major nutrients [29, 30] (see *Annex I*). Two experimentation media were used, Talaquil and 10 mM MOPS (3-morpholine propanesulfonic acid) pH 7.5 adjusted with NaOH.

Phosphate Buffer (PBS) was used to prepare the water for the Ebro River experiments with 1 L Milli-Q water®, 2 g $Na_2HPO_4$ and 0.44 g $NaH_2PO_4 \cdot H_2O$ buffered at pH 7.5.

Glutaraldehide 2.5% were used in a PBS solution for the fixation process of the algae.

## 3.2 Synthesis of $Ru(phen)_3$:$SiO_2$ NPs

$Ru(phen)_3$:$SiO_2$ NPs were synthesized using a *sol–gel* process [31] as it is represented in Figure 5. 23 mL of absolute ethanol, 1.5 mL of $NH_4OH$ solution and 0.5 mL of an aqueous solution (10 mg $mL^{-1}$) of $Ru(phen)_3Cl_2$ were stirred in the dark. After 10 min, 5 mL of a 2:3 TEOS:EtOH mixture was added and kept under stirring for 1 h [32]. The obtained suspension was subjected to ultrasonic stirring for 10 min, followed by several cycles of centrifugation (10000 rpm, 10 min), washing in EtOH and sonication (80 W, 2 min). $Ru(phen)_3$:$SiO_2$ NPs and supernatant were stored in the dark.

In the cases that solid particles are required, the suspensions have been subjected to a lyophilization process. Briefly, the nanoparticles were suspended in water. Then the suspension was freezed and sublimated at low pressure and temperature. The suspensions of nanoparticles were frozen with liquid nitrogen and introduced in a freeze-drier *LyoQuest-55 Telstar* at 0.1 mbar and -52 ºC.

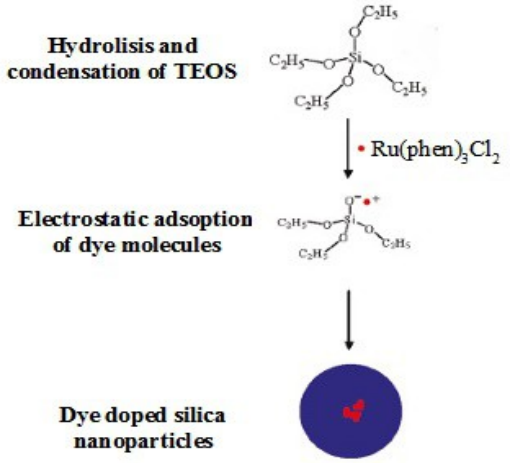


**Figure 5. Schematic illustration of the silica species at different stage of the Stöber reaction and the final situation of the dye molecules added in the particles. (Adapted Image [32])**

## 3.3 Characterization techniques

### *3.3.1 Gravimetric analysis*

The concentration of different nanoparticle suspensions has been determined by gravimetric analysis. This method consists in determining the mass of the remaining dry residue, after solvent evaporation, in a known volume suspension. It is a simple procedure where three aliquots of 0.2 mL are deposited in aluminum crucibles, which have been previously weighed. The solvent has been evaporated at Room Temperature after one day. Then, the mass of the remaining dry residue has been weighted in a scale *MYA 5/2Y Ragwag,* precision 1 µg. In order to minimize the errors associated with the scale, three measurements of each crucible have been made, using as final result the average value.

### *3.3.2 Photo Correlation Spectroscopy*

Dynamic Light Scattering (DLS) measures the Brownian motion of the particles by collecting scattered light that is produced when the dipole changes due to the oscillation induced by an incident photon. So it detects the changes of light intensity, which changes along the time. All the motions and measurements are described by correlations functions, and those correlation functions are related to the hydrodynamic diameter of the nanoparticles in the colloidal.

Also, ζ-potential of nanoparticles in aqueous media has been measured. This characterization technique allows determining the surface charge of the nanoparticles in solution.

Nanoparticles have a surface charge that attracts a thin ions layer of opposite charge. This double layer of ions travels with the nanoparticle as it diffuses throughout the solution. The magnitude of the ζ-potential is related to the colloidal stability. Nanoparticles with ζ-potential values greater that +30 mV or less than -30 mV typically have high degrees of stability. Dispersions with low ζ-potential value will eventually aggregate due to Van der Waal interparticle attractions. ζ-potential is an important tool for understanding the state of the nanoparticle surface and predicting the long term stability of the nanoparticles [28].

The hydrodynamic nanoparticle size and ζ-potential in aqueous media were determined by dynamic light scattering (DLS) with *Brookhaven Instruments 90Plus.* For ζ-potential measurements, ZetaPALS configuration was chosen.

### *3.3.3 Spectrophotometry*

It is a technique based on measuring the light intensity that is emitted by the sample when this one is irradiated at certain wavelength. This process is called fluorescence. Fluorescence is the ability of some substances to absorb electromagnetic radiation at certain wavelengths and emit it in a different one.

The fluorescence emission of $Ru(phen)_3$:$SiO_2$ NPs was analyzed with a *Perkin-Elmer LS 55 Fluorescence spectrometer.* The absorption and emission wavelengths were respectively 448 and 595 nm for $Ru(phen)_3$:$SiO_2$ at 25°C. The scan speed was set at 200 nm $min^{-1}$ with a 7.5 nm grid monochromator. Samples were dispersed in different aquatic media.

Moreover, the fluorescence emission of the different aquatic media in absence of $Ru(phen)_3$:$SiO_2$ nanoparticles was measured 3 times to obtain the blank value.

### *3.3.4 Electron microscopies*

The size, composition and morphology of nanoparticles were characterized by means of electron microscopy techniques.

Transmission electron microscopy (TEM) images were taken using a *Tecnai T20* (*FEI Co., Hillsboro, OR*) electron microscope at 200 kV. The samples have been deposited on FCF200-Cu grids. Statistical particle size-distributions histograms were obtained from TEM images using ImageJ processing software with a number of measured particles (N) of more than 75 in every

image.

Scanning electron microscopy (SEM) was used in order to determine the morphology and composition of the samples. Images were taken using *Cryogenic Dual Beam Nova 200*. The internal distribution of the sample was determined using a Focused Ion Beam, which allows cross sections of the sample. Moreover, *CSEM-FEG INSPECT F50* was used; this equipment allows a fast and simple use, in order to get images of NPs after exposure in environmental relevant conditions. Both instruments allow chemical analysis by means of X-ray Energy Dispersion Spectroscopy (EDS).

Furthermore, SEM analysis of the algae cultures required a previous fixation process in order to maintain its properties unaltered after the incubation experiments. This fixation process have been tuned and optimized especially for this very project. Briefly; right after finishing the incubation experiment the algae sample was centrifuged (2500 rpm, 10 min), then 500 µL glutaraldehide 2.5 % was added to the pellet. After 1.5 h the pellet was purified by several cycles of centrifugation (4000 rpm, 1 min, *MicroCentrifuge Heraeus Pico 17*) washing with 500 µL, 10 mM MOPS. After this fixation process it is necessary to dehydrate the sample and cover it with 13-nm layer of Au-Pd by sputtering, so the sample would be electricity conductor and it could be introduced into the instrument.

## 3.4 Safety and environmental impact of ENMs

### *3.4.1 Surface contamination assessment*

Nanoparticles released to the airborne can be deposited on working areas [33], in order to evaluate this surface contamination a new surface sampling protocol was developed in this project. It consisted on the following procedure:

1. Glass coverslips are evenly distributed on the area under study.

2. Nanomaterial released to the airborne is deposited on the coverslips located in the survey area.

3. The glass coverslips are recovered and the ENPs deposited are resuspended in 5 mL of water.

4. The collected matter is further analyzed by spectrofluorimetry to determine the concentration of $Ru(phen)_3$:$SiO_2$ NPs.

In this regard, a fast screening method for surface contamination has been proposed for the $SiO_2$ NPs that end up on the top of those glass coverslips. To do this, different concentrations of labelled $SiO_2$ nanoparticles were mixed with different concentrations of non-labeled $SiO_2$ nanoparticles (15 nm, Sigma Aldrich), and they have been detected by spectrofluorimetry and visual inspection under LED illumination so the scope of each procedure can be obtained.

As a proof of concept, fluorescent labelled $SiO_2$ NPs were manipulated in the laboratory, and the contamination of work surfaces was quantitatively assessed. Two types of experiments were performed to monitor nanoparticle deposition during nanopowder manipulation as potential contamination sources: (1) gently pouring and (2) transferring from one beaker to another using a spatula. Pouring nanopowder between two beakers was performed, because it has been addressed as a potential source of nanoparticle emission in laboratory environments [16], and both are very common laboratory operations. Experiments were carried out handling 300 mg of $Ru(phen)_3$:$SiO_2$ NPs between two 20 mL-beakers.

Qualitative detection was achieved by visual inspection of the study area under UV light and quantitative analysis of the deposited nanoparticulate matter was performed by spectrofluorimetry analysis.

Figure 6 shows the glass coverslips distribution. The inner ring correspond to A position; from A the outer distributions have been draw in an hexagon pattern being B, C, D, E, F and G, which differ from A; 2.5, 5, 10, 20, 30 and 40 cm respectively. Each ring has 6 equidistant samples distributed in radial geometry.

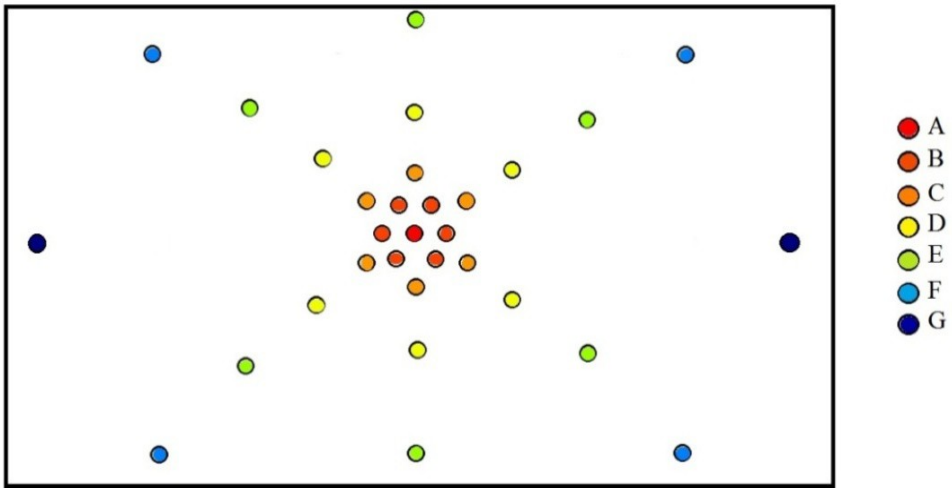


**Figure 6. Glass coverslips distribution for surface contamination assessment in a studied area of 30×40 cm.**

### *3.4.2 Algal culture and photosynthetic yield measurements*

*Chlamydomonas reinhardtii* (wild type, CC-125) were cultured under controlled conditions [29, 30, 34, 35 and 36]. Algae culture were grown in glass Erlenmeyer flask in Talaquil standard growth medium at 25 °C, under continuous illumination of 120 μE $m^{-2}$ $s^{-1}$ Photosinthetically Active Radiation (*PAR*), provided by cool white fluorescent lamps and were shaken at 90 rpm, in a *HT Infors* shaker. Algae culture were acclimatized to the growth medium by transferring algae inoculums of exponentially growing phase to the growth medium in at least two successive batch cultures. Details of algal cells such as typical growth curve, morphology and internal structure images can be found in *Annex I*.

In order to determine the nanoparticle effects on the algal cells, the growth and photosynthetic yield were monitored during the exposure test. To this end, two parameters have been measured:

a. **Optical Density** (OD) was selected as measure of algal growth. Optical Density is directly proportional to the concentration of algal cells - or cells number - in the medium. OD measures the absorbance of light due to the presence of pigments in algal cells. The OD was measured by a *Spectrophotometer Helios α Avantec (Thermo Electron Corporation)* at λ 685 nm [37]. These tests are generally used to determine the toxic effects of substances on algae growth, being OD values an indicator of inhibition algae growth.

b. **Photosynthetic yield** was chosen as a toxicity end point parameter because toxic effects are measurable upon short-term exposure, thus avoiding accumulation of secreted biomolecules that could be toxic for the algal cells and distort the measured results. The algal photosynthetic yield of the photosystem II in light was measured by fluorimetry using a *MINI-PAM Portable chlorophyl parameter (Heinz Walz GmbH)*. Fluorimetry measurements were done at light intensities similar to those used during growth and exposure (120 μE $m^{-2}$ $s^{-1}$ PAR radiation) under continuous shaking. The yield reflects the efficiency of the photochemical energy conversion process [38].

For the exposure test to ENPs, algae culture was synchronized to the final lineal growth of the algae exponential growth phase. Experimental cell were obtained by centrifuging (1500g, 10 min) and then resuspending the cell pellet in the appropriate volume of experimental media: 10 mM MOPS adjusted 7.5 pH with NaOH for short-term experiments (4h), or Talaquil for long-term experiments (72h). The cell densities were $6\times10^5$ cells $mL^{-1}$ (0.15 $OD_{685}$) or, $1\times10^5$ cells $mL^{-1}$ (0.05 $OD_{685}$) respectively.

The exposure medium consisted of stock solutions of 10 mM MOPS (adjusted 7.5 pH with NaOH). Experiments, ranged from 0 to 400 ppm NPs, were prepared in 25-mL Erlenmeyer flasks immediately before each experiment. Algal cultures of the appropriated density were added.

### *3.4.3 Aging of $Ru(phen)_3$:$SiO_2$ NPs: watershed of Ebro River case study*

The Ebro River basin was selected as real-life exposure scenario. Ebro River is one of the most abundant rivers of the Iberian Peninsula with a flow rate of approximately 8832 $hm^3$/year [39]. The river is usually used as a supply of water for agriculture, cattle breeding (89.3 %), domestic (7.2 %) and industrial activities (3.5 %) according to different studies [40]. In addition, the river receives domestic and industrial wastewater from numerous minor settlements along its path. There are different sampling stations from the National Water Quality Control Network (ICA Network) along its basin. The data used in this study is part of the database maintained by the Spanish Ministry of the Environment and were summarized by Bouza-Deaño et al. 2008 [40].

Considering the complexity and variability of natural water chemistry in location and time, three sample sites were selected (Figure 7) as models to prepare the water matrices.

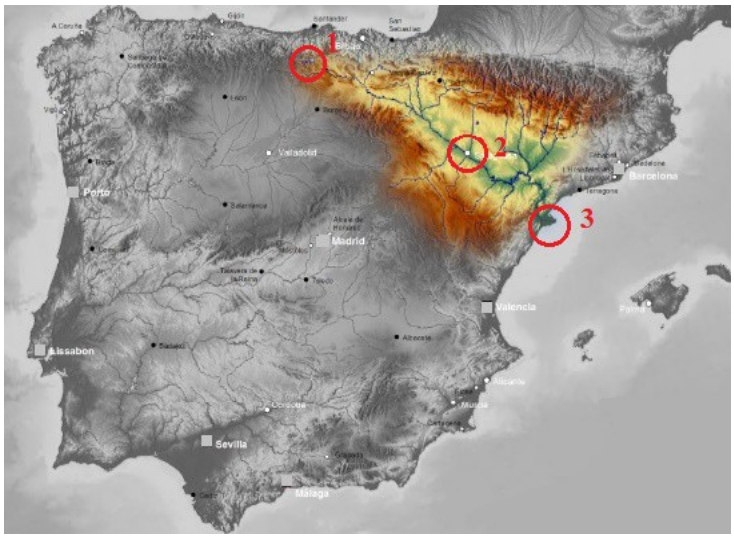


**Figure 7. Map of Ebro river basin in Spain showing the sampling sites on red circle; 1. Source: Cereceda (Site 1); 2. Middle point: Zaragoza (Site 7); 3. Mouth: Tortosa (Site 13). (Adapted image [41])**

Effects of three different sources that alter the water quality were addressed individually: *geogenic* ($SO_4^{2-}$, $Ca^{2+}$, $Na^+$), *turbidity* (Total Suspended Solids, TSS) and *antropogenic* ($NO_3^-$).

Table 1 summarized the composition of diverse aqueous matrices – prepared in PBS buffer

to keep a constant pH 7.5 – used in this study to mimic the real conditions. According to Table 1, nine different aqueous media were prepared, which were replicated three times so it could be exposed under three different conditions: (1) UV light (320 – 400 nm), (2) PAR light (400 – 700 nm), and (3) darkness. For instance, regarding the geogenic factor (F1), three suspensions of 50 ppm of $Ru(phen)_3$:$SiO_2$ NPs were prepared, one for each sampling site (S1, S7, S13) taking into account the parameters in each site.

It was also considered a water sample of Ebro River (extracted in Zaragoza, Aragon, Spain 23/06/2017. Physicochemical analysis of the sample is shown in *Annex II*). Suspensions of 50 ppm of $Ru(phen)_3$:$SiO_2$ NPs were prepared.

These suspensions were introduced in open glasses of 8 cm diameter, to improve the exposure to light, except for darkness experiments that were closed. In order to keep the same volume along the experiment, Milli-Q water® was added after daily evaporation.

$Ru(phen)_3$:$SiO_2$ NPs were aged during 7 days in those aqueous matrices under the conditions described above. The samples were kept at 15 ºC under orbital stirring (100 rpm) in an incubation chamber.

**Table 1. Summary of parameters for the study of environmental effects on $Ru(phen)_3$: $SiO_2$ NPs. Units of the parameters expressed in ppm.**

| *Factor* | *Type* | *Parameters* | *Site 1* | *Site 7* | *Site 13* |
|---|---|---|---|---|---|
| *F1* | *Geogenic* | $Ca^{2+}$ | 50 | 150 | 100 |
| | | $Na^{+}$ | 25 | 218 | 193 |
| | | $SO_4^{2-}$ | 25 | 218 | 193 |
| *F2* | *Tubidity* | TSS | 9 | 75 | 10 |
| *F3* | *Antropogenic* | $NO_3^{-}$ | 4 | 19 | 10 |

In this work, the aging of $Ru(phen)_3$:$SiO_2$ NPs in aqueous media was investigated. The aging experiments were focused on Ebro River basin case study and changes in (*i*) the structure of the nanoparticles (by SEM); (*ii*) the fluorescent emission at 595 nm; and (*iii*) in the ζ-potential was analyzed.

# 4. RESULTS AND DISCUSSION

## 4.1 Characterization of pristine labelled $Ru(phen)_3$:$SiO_2$ NPs

The fluorescently labelled $Ru(phen)_3$:$SiO_2$ NPs showed an spherical shape with a mean size of 84.5 ± 13 nm (see TEM and SEM pictures in Figure 8).

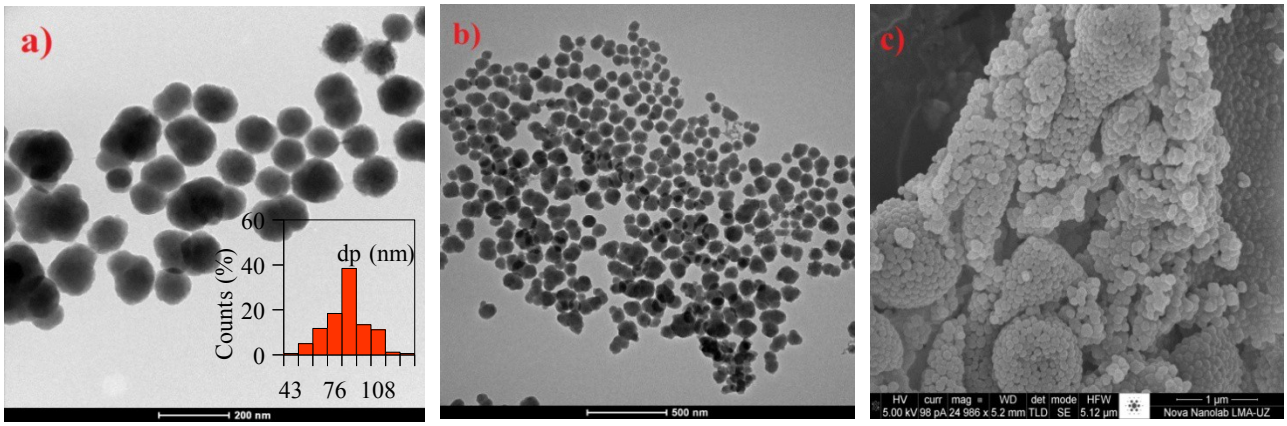


**Figure 8. TEM (a) (b) and SEM (c) images of $Ru(phen)_2$-labelled $SiO_2$ NPs. The histogram represents the nanoparticle size distribution, obtained from TEM images with N>180.**

The synthesis of these nanoparticles was done according to the method described in Section 3.2, obtaining a slightly polydisperse sample. The hydrodynamic diameter of the fluorescent nanoparticles is distributed around 100 nm (Figure 9) showing a low polydispersity between 0.1 – 0.15.

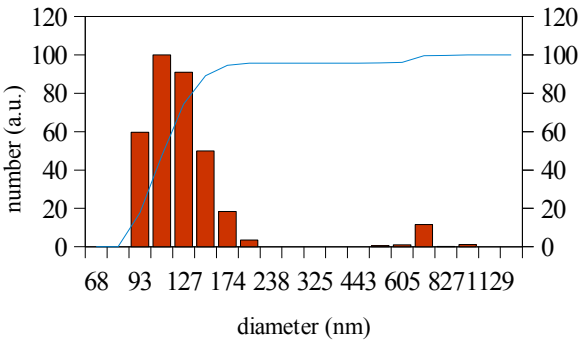


**Figure 9. Hydrodynamic diameter of $Ru(phen)_3$:$SiO_2$ NPs.**

The surface of the hydrodynamic shear of fluorescent $SiO_2$ NPs showed a negative electrostatic potential in almost the entire pH range as it is observed in Figure 10. From pH 6, NPs showed ζ-potential values under - 30 mV, which implies high colloidal stability in aqueous natural

environments. Its measurements can also provide valuable information regarding the fate, behavior and toxicity of nanomaterials in environmental and biological systems [42].

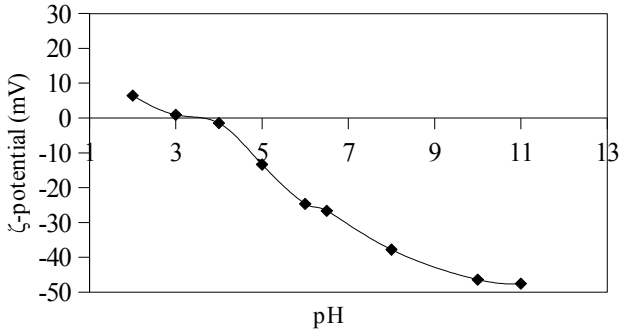


**Figure 10. ζ-Potential vs. pH plot of a typical 20 ppm aqueous suspension of $Ru(phen)_3$:$SiO_2$ NPs showing the negative surface charge beyond ~ pH 4 (point of zero charge, PZC).**

Such nanoparticles showed fluorescent emission spectra at 595 nm (Figure 11), which is translated into reddish colored nanoparticles. The fluorescent emission of the labelled nanoparticles was stable in diverse environments [24, 28] after a period of stabilization. For this reason, the fluorescent nanoparticles were aged at RT and sunlight during 24 h until the fluorescent emission was in the steady region.

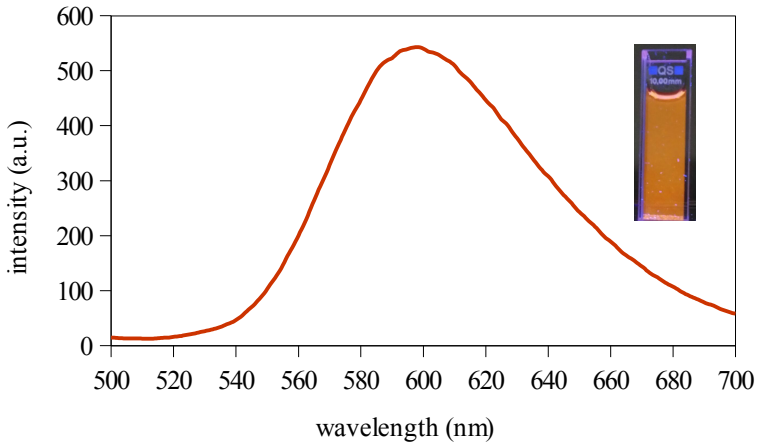


**Figure 11. Typical fluorescent emission spectrum of $Ru(phen)_3$:$SiO_2$ NPs in aqueous dispersion at 50 ppm. Emission was excited by laser irradiation at 448 nm and scanned with a 7.5 nm grid monochromator. The inset shows an image of the 50 ppm $Ru(phen)_3$:$SiO_2$ NPs suspension under irradiation using UV light.**

## 4.2 Surface contamination assessment

The appropriate surface sampling procedure will be crucial for the correct estimation of the likelihood of dermal exposures to engineered nanomaterials in the workplace. To address this issue, a new surface sampling procedure has been developed in this project (see Section 3.4.1) (Figure 12). Briefly, glass coverslip were evenly distributed over the study area. After the NPs were deposited on the surface, the coverslips were recovered and $Ru(phen)_3$:$SiO_2$ NPs were resuspended in 5 mL of water. This suspension was tested by spectrofluorimetry, and the intensity of the emission peak obtained was interpolated in the calibration curve (see *Annex III*) getting the concentration of that suspension, and so the amount of $Ru(phen)_3$:$SiO_2$ NPs. This process presents a recovery percentage of 96.2 ± 4.5% of NPs (More details are shown in *Annex IV*).

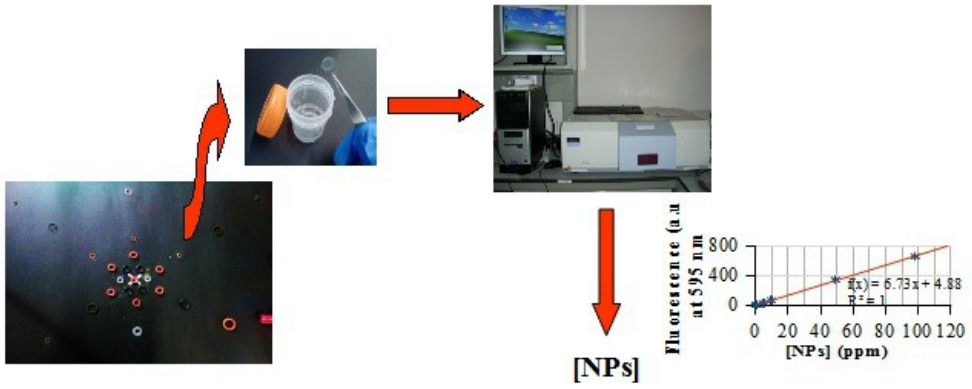


**Figure 12. Schematic representation of sampling procedure to assess fluorescent NPs surface contamination.**

Based on the foregoing, a fast screening method for surface contamination has been proposed. First, different aqueous suspension of labelled $Ru(phen)_3$:$SiO_2$ NPs are mixed with different amount of non-labelled $SiO_2$ NPs. Then 0.1 mL of each suspension was deposited in a glass coverslip given the following pattern: a matrix shown in Figures 13 and 14 has been made from samples with a decreasing concentration of labelled $Ru(phen)_3$:$SiO_2$ NPs (horizontal), mixed with non-labelled $SiO_2$ NPs (vertical). The dry solid deposited in each glass coverslip was screening by visual inspection under LED light and laser.

Figure 13 shows the matrix where each glass coverslip has been illuminated with a laser (wavelength of 405 nm). Moreover, Figure 14 shows the same matrix, but illuminated under LED light also 405 nm. These pictures show the scope of the technique, being that the orange/reddish colors are due to the fluorescence of the labelled nanoparticles, that confirms its presence. On the other hand, bluish colors are the result of absence of nanoparticles. Thanks to this, it is possible to

detect the presence of around 40 ng of NPs under laser, and 200 ng under LED.

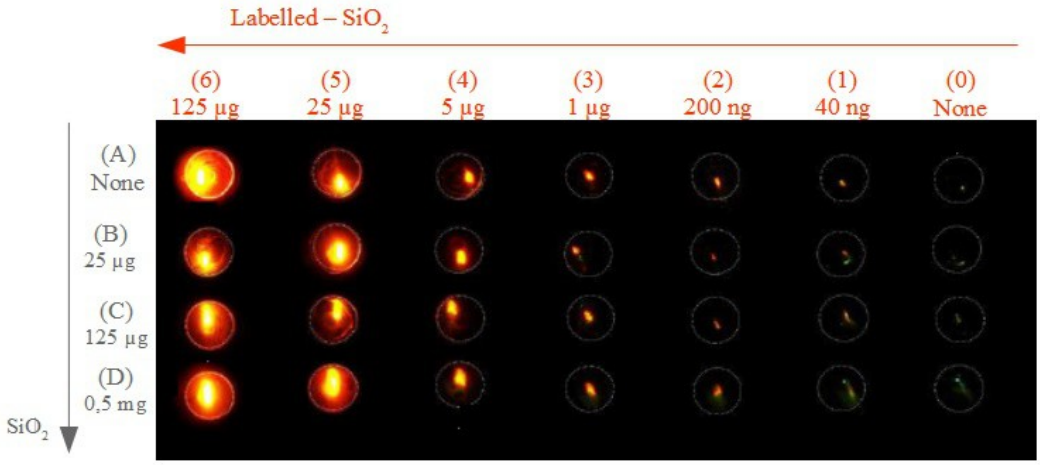


**Figure 13. Image illuminated by laser 405 nm. The numbers around the picture shows the mass of nanoparticles deposited on each coverslip.**

**Figure 14. Image illuminated by LED 405 nm.**

After this fast screening under selected light, the $SiO_2$ nanoparticles deposited on these glass coverslips was analyzed by spectrofluorimetry. Sufficient analyte concentration must be present to produce an analytical signal that can reliably be distinguished from "analytical noise," the signal produced in the absence of analyte. An approximate estimation of LoD can often be obtained from the signal-to-noise (S/N) ratio of the analyte signal measured in the matrix. A (S/N) ratio of 3 is generally considered acceptable when estimating the detection limit [24]. The (S/N) ratios from fluorimetry analysis of the $Ru(phen)_3$:$SiO_2$ NPs recovered were collected in Table 2. If the (S/N) ratio is over 3, nanoparticles could be detected (orange cells). Otherwise the absence of nanoparticles was considered (blue cells). In each case, the blanks corresponded to suspensions of non-labelled $SiO_2$ NPs according to the concentrations mentioned in Figure 13 (A: none, B: 25 µg, C; 125 µg and D: 0.5 µg).

**Table 2. Signal-to-noise ratio of each sample or coverslip measured by spectrofluorimetry.**

| Labelled NPs/ non-labelled | 125 µg | 25 µg | 5 µg | 1 µg | 200 ng | 40 ng | None |
|---|---|---|---|---|---|---|---|
| None | 48.4 | 11.2 | 3.3 | 1.6 | 1.5 | 1.3 | 1 |
| 25 µg | 32.6 | 8.7 | 2.8 | 1.4 | 1.2 | 1.1 | 1 |
| 125 µg | 13.2 | 4.1 | 1.9 | 1.2 | 1.1 | 1 | 1 |
| 0.5 mg | 8.8 | 2.7 | 1.4 | 1.1 | 1.1 | 1.1 | 1 |

This procedure has allowed distinguish fluorescent labelled NPs from background nanosized matter already present in the sampling environment. Moreover, it has allowed identifying the fluorescent nanoparticles in the sampling environment down to levels of 0.62 ppm.

Finally, this surface sampling procedure was tested while handling nanomaterials in the laboratory, in order to quantitatively assess the surface contamination. Two different tasks were analyzed: pouring and transferring nanopowders. The results of these tasks can be seen in Figure 15.

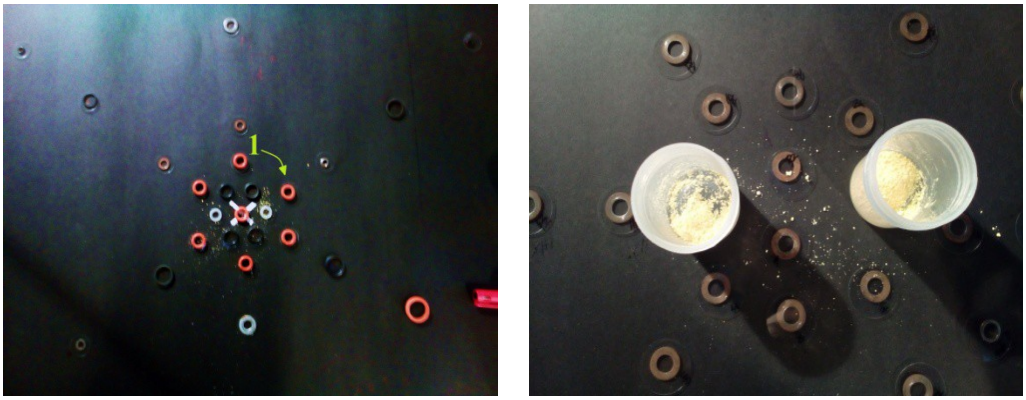


**Figure 15. Visible results of pouring (left) and transferring (right).**

Afterwards, the coverslips were retrieved and fluorescent NPs were resuspended in water in accordance with the sampling method developed. These suspensions have been measured by spectrofluorimetry and results are summarized in Table 3 and 4 (see also *Annex V*). In these tables is observed the area that has been contaminated during the simulation of both pouring and transferring. In other words, it is possible to quickly know the distance that the nanomaterial can reach, and consequently contaminate, for these common laboratory tasks. Being point A the closest location to NPs emission source and point G the farthest one, as disclosed in the spectrofluorimetry

results. The number corresponds to the coverslips distributed clockwise around each position, see Figure 15.

**Table 3. Spectrofluorimetry measurements. ENPs (µg) recovery from pouring experiment.**

| | 1 | 2 | 3 | 4 | 5 | 6 |
|---|---|---|---|---|---|---|
| **A** | 18.3 ± 0.2 | | | | | |
| **B** | 28.2 ± 0.8 | 218.2 ± 1.7 | 34.7 ± 0.4 | 14.3 ± 0.3 | 37 ± 0.4 | 1.9 ± 0.4 |
| **C** | -- | 3.9 ± 0.01 | 5.9 ± 0.3 | 13 ± 0.1 | 37.2 ± 0.4 | 0.9 ± 0.1 |
| **D** | -- | 10.4 ± 0.4 | 3.2 ± 0.6 | -- | 0.7 ± 0.1 | -- |
| **E** | 0.6 ± 0.4 | 2.2 ± 0.5 | 0.7 ± 0.8 | 4.5 ± 1 | 2.5 ± 0.3 | 1.7 ± 0.6 |
| **F** | 2.5 ± 0.9 | 3 ± 0.5 | 0.1 ± 0.2 | 0.8 ± 0.3 | | |
| **G** | 2.6 ± 0.6 | 1.5 ± 0.5 | | | | |

**Table 4. Spectrofluorimetry measurements. ENPs (µg) recovery from transferring experiment.**

| | 1 | 2 | 3 | 4 | 5 | 6 |
|---|---|---|---|---|---|---|
| **A** | 428.1 ± 3.4 | | | | | |
| **B** | 1 ± 0.1 | -- | 18.9 ± 0.8 | 10.7 ± 1.1 | 3.2 ± 0.1 | 0.7 ± 0.1 |
| **C** | -- | 1.5 ± 0.1 | -- | 4.4 ± 0.3 | 0.5 ± 0.1 | -- |
| **D** | -- | 1 ± 0.3 | -- | 1.3 ± 0.7 | 1.1 ± 0.1 | -- |
| **E** | -- | -- | -- | -- | -- | -- |
| **F** | -- | -- | -- | -- | | |
| **G** | -- | -- | | | | |

## 4.3 Environmental impact

### *4.3.1 Algae toxicity*

The effects of $Ru(phen)_3$:$SiO_2$ NPs was tested over algae *Chlamydomonas reinhardtii*. As first approach, a short-term exposure test was done. The algal cells was exposed during 4 h to a concentration of 50 ppm of $Ru(phen)_3$:$SiO_2$ NPs (Figure 16). This experiment does not provide enough information since any toxic effects or changes in cells morphology were found.

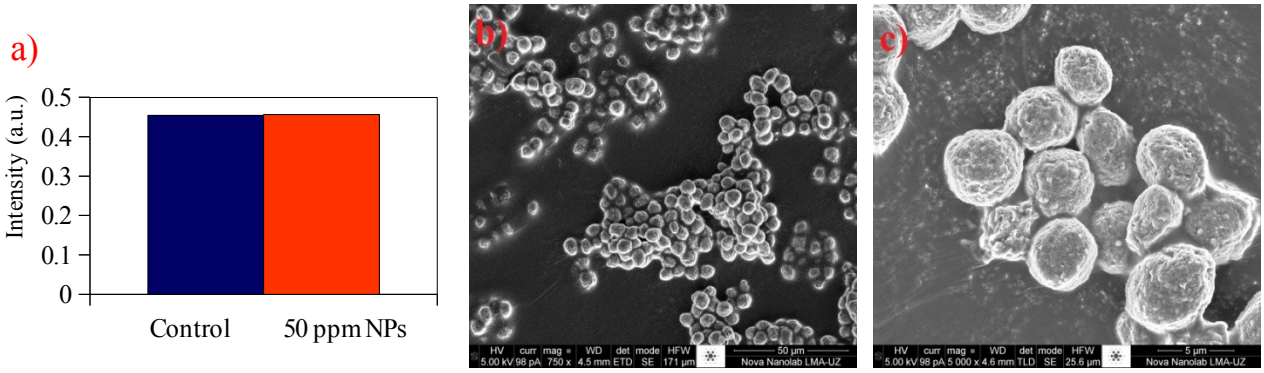


**Figure 16. (a) Photosynthetic yield changes respect the control (SD<0.04) (left) and (b) algae appearance before and (c) after 4 h exposure test.**

Therefore, long-term exposure test was conducted. In that case, the algae culture was incubated with different nanoparticles concentration during one algal growth phase (72 h). The algal growth in terms of optical density ($OD_{685}$) and the photosynthetic yield were monitored during the long-term exposure test. Figure 17 shows the percentage variation of $OD_{685}$ with respect to the control at 24 h of exposure. Higher inhibition on the algae growth rate ($\Delta(OD_{685})$) is observed with higher nanoparticle concentration, up to 100 ppm. Whereas for 400 ppm of NPs, $\Delta(OD_{685})$ slightly fell and a less toxic effects on the algal cells were observed. This may be attributed to the aggregation of NPs at higher concentrations and thus less bioavailability to interact with algal cells surface [43].

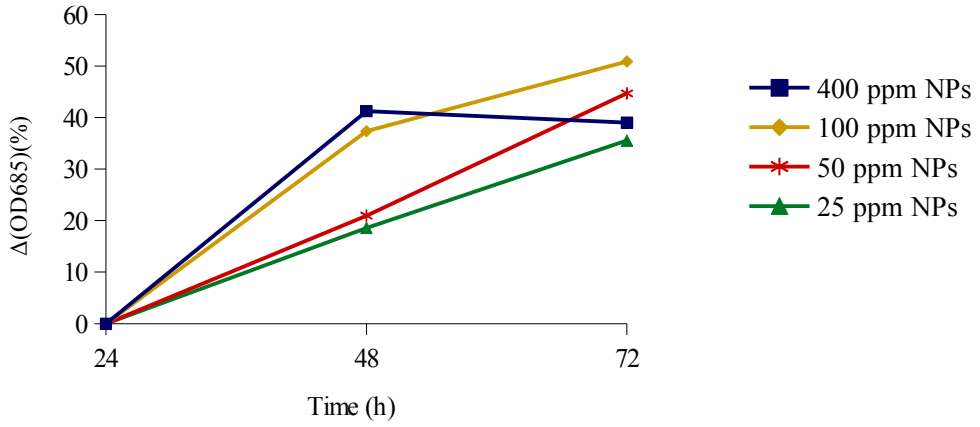


**Figure 17. $\Delta(OD_{685})$ % respect to the control, or sample in absence of nanoparticles, at different NP concentrations. Data were previously normalized respect 24 h data.**

Regarding the photosynthetic yield, no significant changes were found, with the exception of exposure test to 50 ppm of $Ru(phen)_3$:$SiO_2$ NPs. In this case, the photosynthetic yield has decreased 32 % respect to the control (see *Annex VI*). Higher concentration did not produce toxic effects, it may be due to higher nanoparticles aggregation, and consequently it reduces the interaction with the surface of the algal cell.

By means of scanning electron microscopy (SEM), algal cell images were taken to visualize how cells have been affected. The morphology of control algal cells, and cells after the long-term exposure test to different nanoparticles concentration, is shown in Figures 18 to 21. Although an inhibition on the algae growth rate was observed, algal cells exposed to 25 and 50 ppm of $Ru(phen)_3$:$SiO_2$ NPs during 72 h did not present any changes in the external morphology and no internalized NPs was found inside the cells (Figure 18).

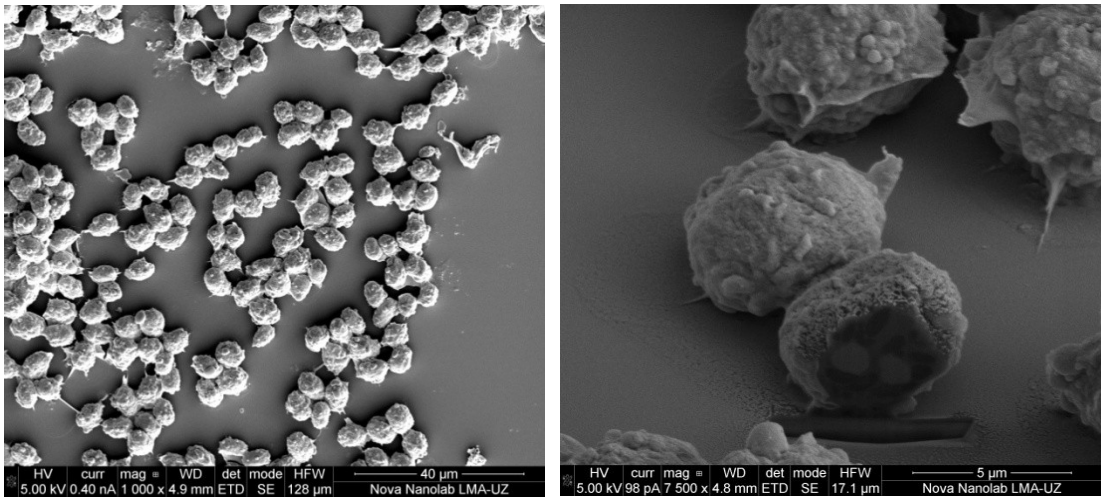


**Figure 18. *C. reinhardtii* SEM images of control (left) and after an exposure test of 72 h to 50 ppm of NPs (right).**

On the other hand, $Ru(phen)_3$:$SiO_2$ NPs aggregates, attached to the cell surface, were observed in algal cell exposed to 100 ppm of NPs during 72 h. While, it seems to affect the algae growth ($OD_{685}$), the morphology of the cells has not changed respect the control, and no internalized NPs were found inside the cells (Figure 19).

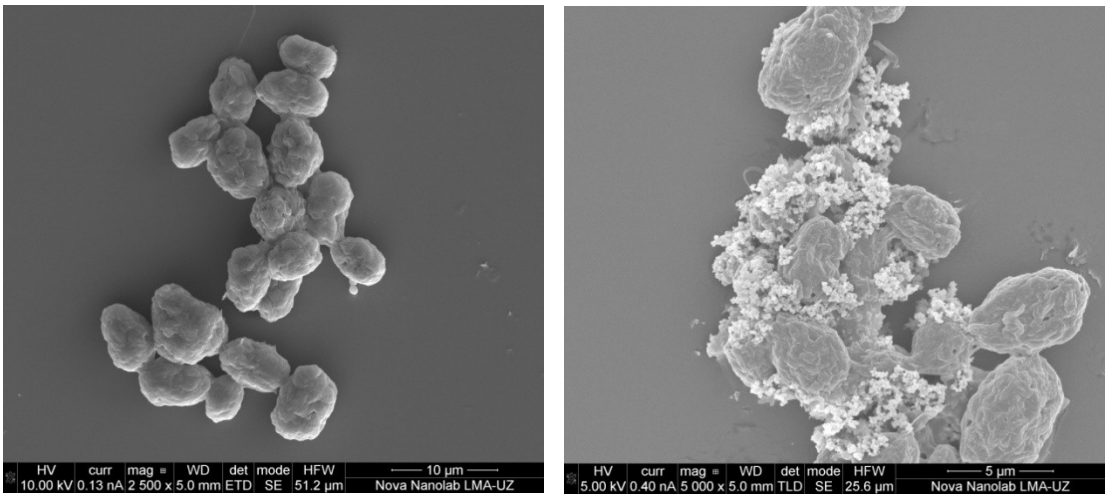


**Figure 19. *C. reinhardtii* SEM images of control (left) and after an exposure test of 72 h to 100 ppm of NPs (right).**

Finally, $Ru(phen)_3$:$SiO_2$ NPs aggregates attached to the cell surface, were seen in algal cell exposed to 400 ppm of NPs during 72 h (Figure 20). Moreover, the morphology was very affected respect to the control (Figure 21); and in that case internalized NPs were found inside the cells, as it is observed in Figure 22. EDS analysis was performed on the nanoparticles that were found inside the cell. It revealed the presence of Si (2.35% Si) (Figure 23).

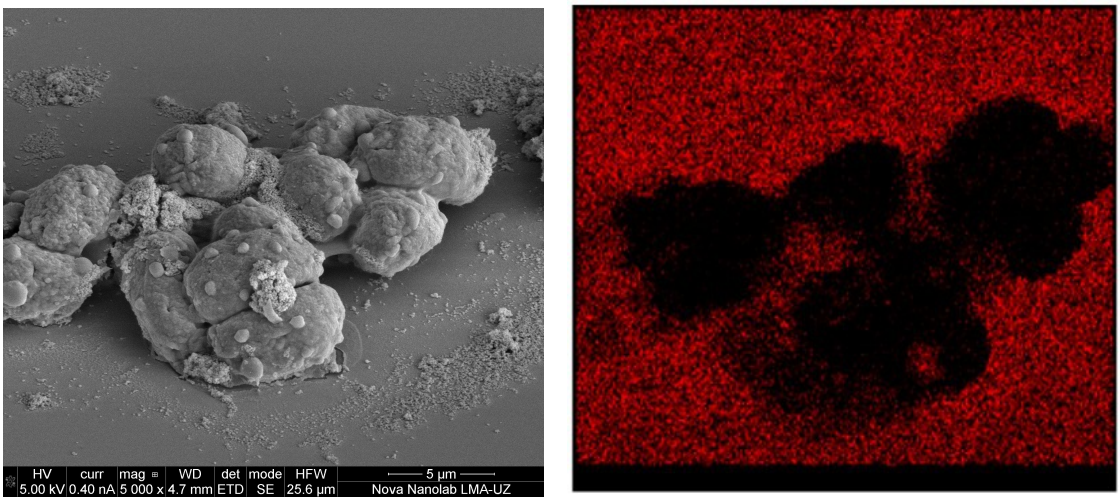


**Figure 20. SEM images of *C. reinhardtii* after 72 h exposed to 400 ppm of NPs (left) and EDS analysis showing in red the Silica present in the sample (right).**

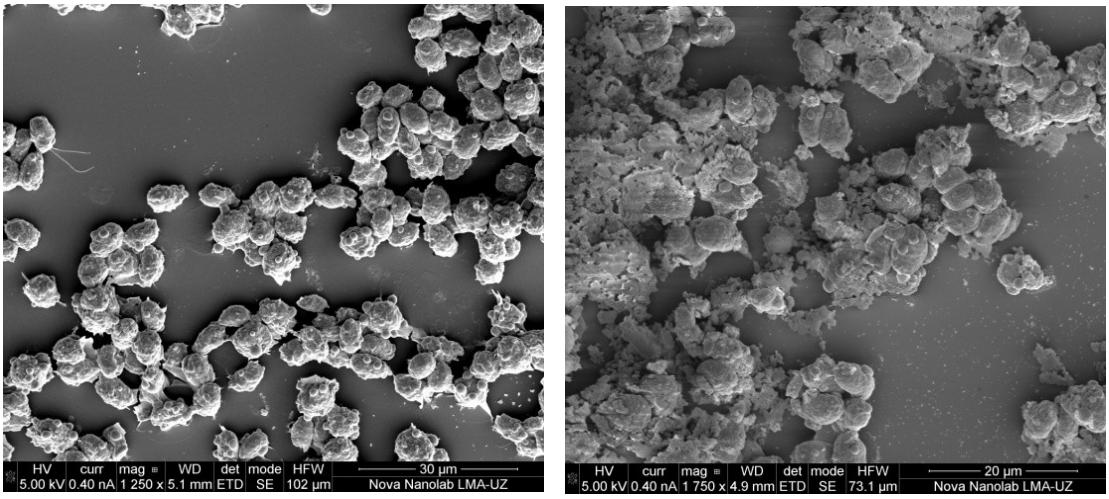


**Figure 21. *C. reinhardtii* SEM images of control (left) and after 72 h (right) exposed to 400 ppm of NPs.**

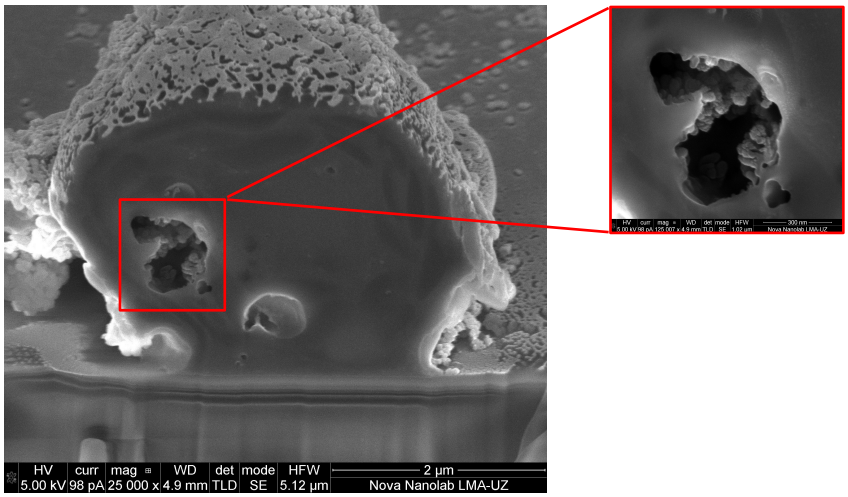


**Figure 22. SEM image of NPs internalized in the cell. *C. reinhardtii* after 72 h exposed to 400 ppm of NPs.**

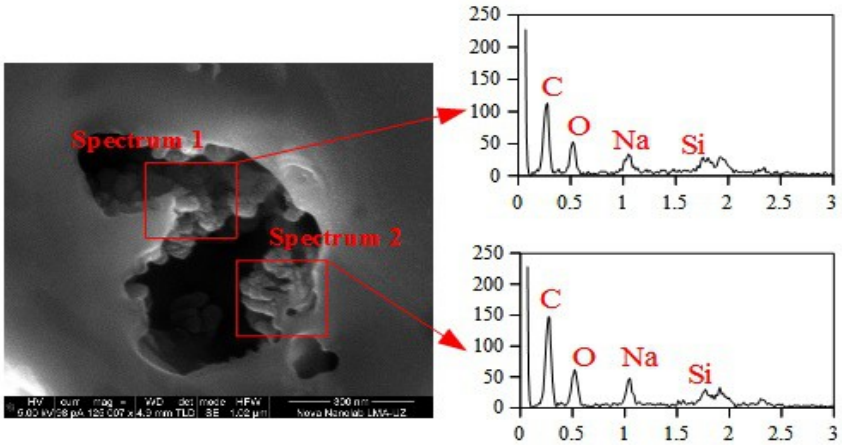


**Figure 23. EDS analysis in the algal cell interior.**

### *4.3.2 Aging of $Ru(phen)_3$:$SiO_2$ NPs*

$Ru(phen)_3$:$SiO_2$ NPs were aged in aqueous matrices prepared according to Table 1, mimicking Ebro River physicochemical characteristics and also in Ebro River freshwater, following the same procedure. Then the $Ru(phen)_3$:$SiO_2$ NPs were characterized attending the changes produced in: (i) the structure of the nanoparticles, (ii) fluorescence and (iii) ζ-potential.

(i) *NPs structure.* SEM images were taken before and after aging the nanoparticles under different conditions. The nanoparticles structure presented no significant changes. But $Ru(phen)_3$:$SiO_2$ NPs tended to form micrometric aggregates (1 – 10 µm) (further information in *Annex VII*).

(ii) *Effects on the NPs fluorescence intensity* (Figure 24) according to three different sources that produce variations in the water quality: *geogenic* ($SO_4^{2-}$, $Ca^{2+}$, $Na^{+}$), *turbidity* (TSS) and *antropogenic* ($NO_3^{-}$). In all the cases, the media produces a fluorescence signal, which has been taken into account. This measure has been rested from the total fluorescence intensity.

Overall, after the exposure test under both UV and PAR light, the fluorescence decrease drastically (Figure 24). This phenomena is due to the quenching of the fluorescence signal of $Ru(phen)_3$ in the outer layers of the nanoparticles [28]. It is not the case of NPs aged under dark conditions, where loss of fluorescence intensity was not so severe. Taking into account the different sources, the geogenic factor was the most relevant in terms of reducing fluorescence intensity. However, the turbidity of the media avoided the loss of fluorescence intensity due to the attenuation of UV and PAR light intensity through the media. It has prevented the quenching of fluorescence emission of the nanoparticles.

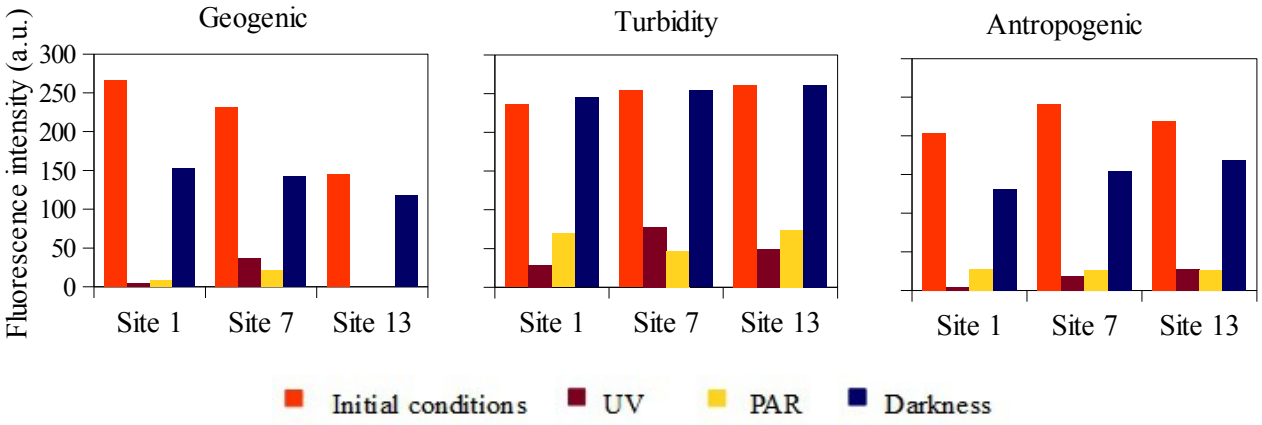


**Figure 24. Changes in fluorescence intensity after 7 days of exposure under UV light, PAR light and dark conditions.**

(iii) *Effects on NPs ζ-potential.* Again, the effects of the three different sources on the ζ-potential of the NPs are shown (Figure 25). In general, it was observed a decrease in ζ-potential, below -30 mV. Consequently, the colloidal stability decreased, and nanoparticles tended to aggregate, as it can be seen in *Annex VII*.

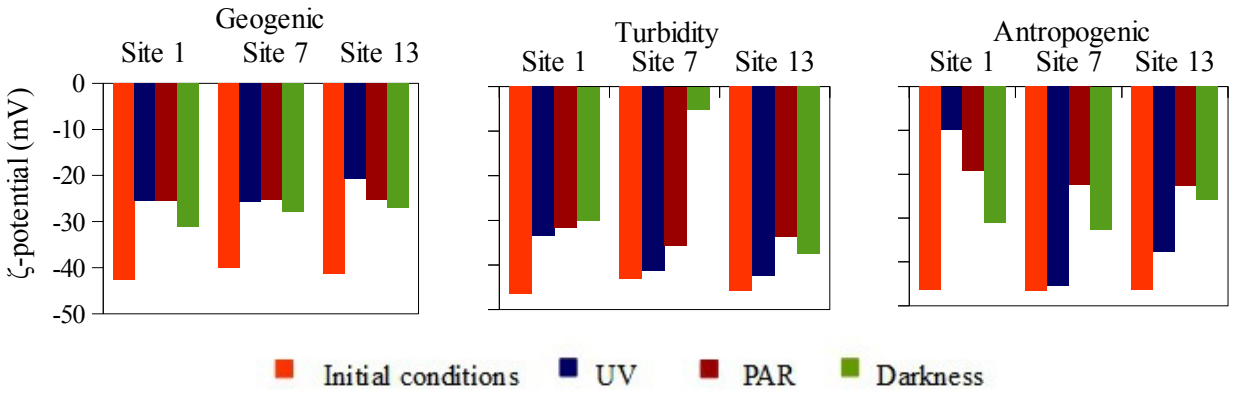


**Figure 25. Changes in ζ-potential after 7 days of exposure under UV light, PAR light and dark conditions.**

Finally, a sample of river water of Ebro River (extracted in Zaragoza, Aragon, Spain 23/06/2017) was used as aging media. Changes in (*i*) the structure of the nanoparticles (by SEM); (*ii*) the fluorescent emission at 595 nm; and (*iii*) in the ζ-potential are shown in Figures 26 and 27. Figure 26 shows the tendency of $Ru(phen)_3$:$SiO_2$ NPs to form micrometric aggregates with the natural organic matter present in the river water.

There was a synergistic effect between the different sources that affect the water quality. Fluorescence intensity of $Ru(phen)_3$:$SiO_2$ NPs has decreased drastically after aging in UV and PAR light conditions as expected from previous tests in the prepared aqueous media. However, the aging in dark conditions has produced a higher decrease in the fluorescence intensity of the NPs, contrary to the previous results in the prepared aqueous matrices. It may be attributed to the complexity of the river aqueous media in comparison to the synthetic ones, in terms of natural organic matter, presence of microorganisms...etc.

As a result of aging $Ru(phen)_3$:$SiO_2$ NPs in Ebro River freshwater, a decrease in ζ-potential, below -15 mV, was observed (Figure 27). Consequently, the colloidal stability decreased, and nanoparticles tended to aggregate with natural organic matter present in the media.

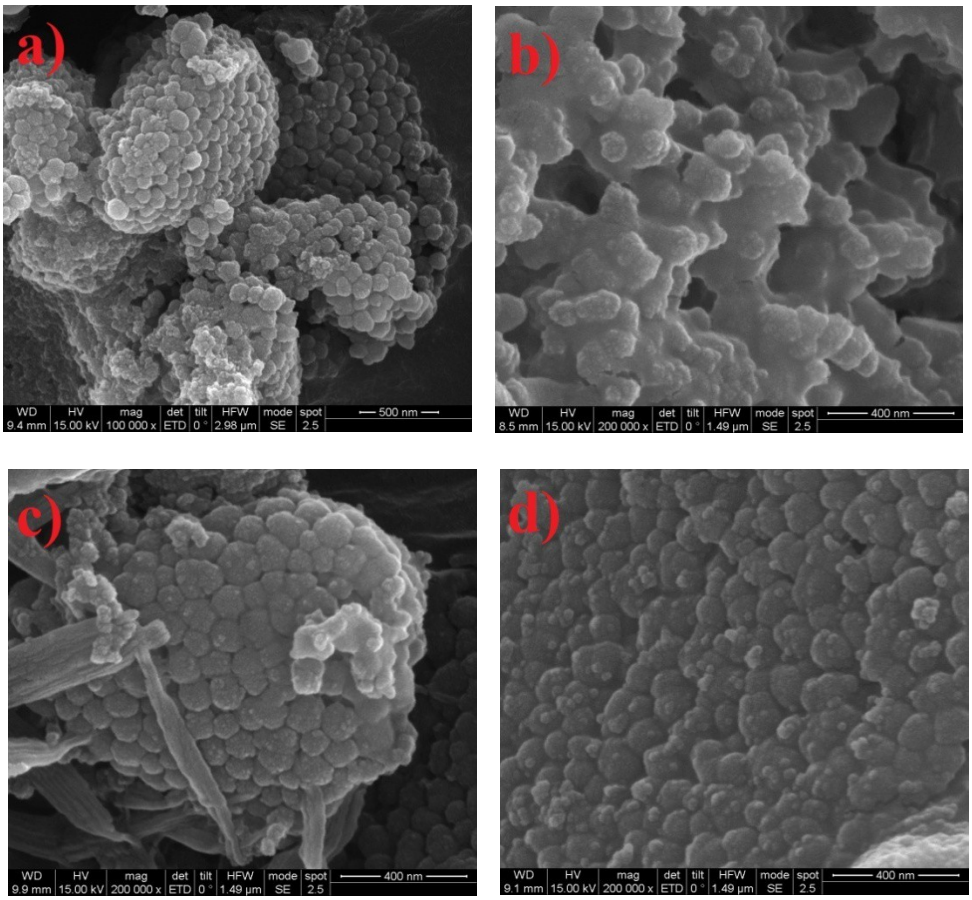


**Figure 26. SEM images of $Ru(phen)_3$:$SiO_2$ NPs in Ebro River freshwater (a) before and after aging test under (b) UV, (c) PAR and (d) dark conditions.**

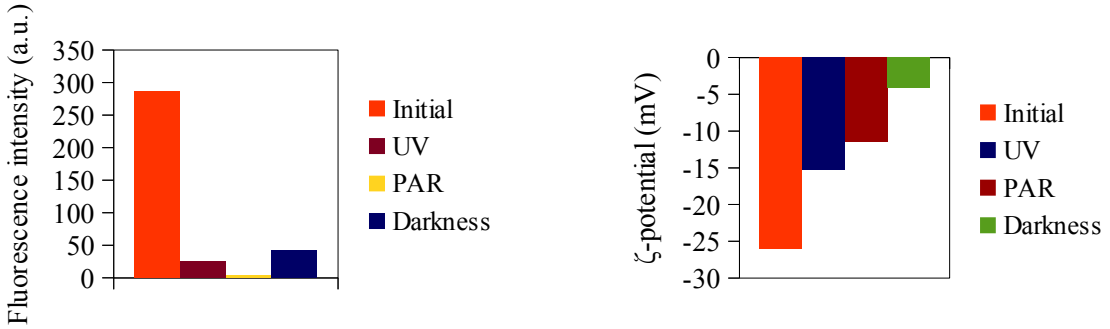


**Figure 27. Fluorescence signal of NPs in Ebro River water (left) and ζ-potential of the particles (right) exposed under different conditions.**

# 5. CONCLUSIONS

$Ru(phen)_3:SiO_2$ nanoparticles can be used as tracers for surface contamination assessment. With the developed method, it is possible to determine the concentration of nanoparticles in the study area, and to visualize the contaminated area during common laboratory operations. The method is quick, accessible and simple to accomplish.

Moreover, these labelled nanoparticles can also be used as tracers in aquatic media. The environmental implications of these labelled nanoparticles have been assessed in algal cells such as *Chlamydomonas reinhardtii*. Although the toxicity of $SiO_2$ NPs is lower than most NPs, it should deserve special concern for the complex interaction of $SiO_2$ NPs and other substance in the environment. The use of $Ru(phen)_3:SiO_2$ NPs allows to assess the adverse effect to aquatic environments.

The aging process of $Ru(phen)_3:SiO_2$ NPs based on the physicochemical conditions of Ebro River basin, has been considered. Although the morphology of $Ru(phen)_3:SiO_2$ NPs has not significantly changed, disturbance in the stability and properties were observed as a consequence of the variations in the ζ-potential and fluorescence. The low stability of NPs after the aging process led to form micrometric aggregations of NPs. Last but not least, the information about the aging process has led to a better understanding in the changes of $Ru(phen)_3:SiO_2$ NPs after aging in Ebro River freshwater.

.

# 6. REFERENCES


**1.** US National Nanotechnology 2006. *http://www.nano.gov/html/facts/whatIsNano.html*

**2.** C. Grimpe and R. Patuelli. *The Annals of Regional Science 46 (3): 419–51, 2011*

**3.** Definition of nanomaterial (2011/696/EU) . *http://ec.europa.eu/environment/chemicals/nanotech/faq/definition_en.htm*

**4.** A. Marmur. *Langmuir, 20 (9), pp 3517-3519. 2004.*

**5.** R. J. Aitken, M. Q. Chaudhry, A. B. A. Boxall, M. Hull. *Occup Med (Lond) (2006) 56 (5): 300-306.*

**6.** HF. Krug and P. Wick. *Angew Chem Int Ed 50:1260–1278 (2011)*

**7.** K. Sovolainen. *Chem Biol Interact. 2013 Sep 5;205(1):A1-5*.

**8.** Finnish Institute of Occupational Health (FIOH) *https://www.ttl.fi/en/*

**9.** Nanotechnology Products Database (NPD). *http://product.statnano.com*

**10.** Luxresearch. 2014 *https://members.luxresearchinc.com/research/report/13748*

**11.** M. E. Vance, T. Kuiken, E. P.Vejerano, S. P. McGinnis, M. F. Hochella, D. Rejeski and M. S. Hull. *Beilstein J. Nanotechnol. 2015, 6, 1769–1780.*

**12.** European Association of Industrial Silica Producers. *http://www.eurosil.eu/silica-and-health*

**13.** F. Piccinno, F. Gottschalk, S. Seeger, B. Nowack. *J Nanopart Res (2012) 14:1109*

**14.** T. L. Rocha, N. C. Mestre, S. M. T. Sabóia-Morais, M. J. Bebianno. *Environ Int. 98 (2017) 1–17*.

**15.** H. F. Krug. *Angew. Chem. Int. Ed. 2014, 53, 12304 – 12319*

**16.** V. Gomez, S. Irusta, F. Balas, N. Navascues, J. Santamaria. *J. of Hazardous Mats. 279 (2014) 75–84*

**17.** S. J. Tsai, E. Ada, J. A. Isaacs, M. J. Ellenbecker. *J Nano. Res (2009) 11:147–161*

**18.** T. Schneider, R. Vermeulen, D. H. Brouwer, J. W. Cherie, H. Kromhout, C. L. Fogh. *Occup Environ Med.1999;56:765–73.*

**19.** M. A. Byrne. *Ann Occup Hyg. 2000; 44(7):523–8.*

**20.** J. A. Shatkin. *CRC Press, Taylor and Francis Group. 2013*

**21.** D. M. Mitrano, S. Motellier, S. Clavaguera, B. Nowack. *Environm. Int. 77 (2015) 132–147*

**22.** N. Lubick. *Environm. Sci. Technol, 2009, 43, 6446-647*

**23.** V. Gomez, A. Clemente, S. Irusta, F. Balas and J. Santamaria. *Environ. Sci.: Nano, 2014, 1, 496*

**24.** A. Clemente, N. Moreno, M. P. Lobera, F. Balas and J. Santamaria. *Environ. Sci. Nano, 2016, 3, 631*

**25.** M. Rennie. *Proc Nutr Soc. 58 (4): 935–44 1999*

**26.** A. D. Dybowska, M. N. Croteau, S. K. Misra, D. Berhanu, S. N. Luoma, P. Christian, P. O'Brien and E. Valsami-Jones. *Environ. Pollut., 2011, 159, 266.*

**27.** N. Neubauer, F. Weis, A. Binder, M. Seipenbusch, G. Kasper. *J. Phys. 2011, 304, 012011.*

**28.** A. Clemente. *PhD Thesis. Zaragoza University. 2017*

**29.** S. Le Faucheur, R. Behra and L. Sigg. *Environ Tox and Chem, Vol. 24, No. 7, pp. 1731–1737, 2005*

**30.** I. Sziva´k, R. Behra , and L. Sigg. *J. Phycol. 45, 427–435 (2009)*

**31.** L. M. Rossi, L. Shi, F. H. Quima and Z. Rosenzweig. *Langmuir, 2005, 21, 4277.*

**32.** D. Zhang, Z. Wu, J. Xu, J. Liang, J. Li, and W. Yang. *Langmuir 2010, 26(9), 6657–6662*

**33.** A. D. Maynard and R. J. Aitken. *Nanotoxicology, 2007; 1(1): 26 41*

**34.** E. Navarro, B. Wagner, N. Odzak, L. Sigg, and R. Behra. *Environ. Sci. Technol 2015.*

**35.** D. D. Wykoff, J. P. Davies, A. Melis, and A. R. Grossman. *Plant Physiol. (1998) 117: 129–139*

**36.** E. Navarro, F. Piccapietra, B Wagner, F Marconi, R. kaegi, L Sigg, R Behra. *Environ. Sci. Tech 2008*

**37.** F. Jia , M. Kacira and K. L. Ogden. *Sensors 2015, 15, 22234-22248.*

**38.** U. Schreiber, W. Bilger and C. Neubauer. *Ecophys. Photosynth; Springer 1994; Vol. 100, pp 49−70*

**39.** Confederación Hidrográfica del Ebro *CHEbro www.chebro.es*

**40.** R. Bouza-Deaño, M. Ternero-Rodrıguez, A.J. Fernandez-Espinosa. *J of Hydrol 2008 361, 227– 239*

**41.** Global Water Forum *http://www.globalwaterforum.org/regions/basins/ebro-basin/*

**42.** G. V. Lowry. *Environ. Sci. Nano, 2016, 3, 953-965*

**43.** C. Wei, Y. Zhang, J. Guo, B. Han, X. Yang, J. Yuan. *J. of Environ Sciences 2010, 22(1) 155–160*